AIAA 94-3336

# Characterization of the Near-Anode Region of a Coaxial MPD Thruster

Kevin D. Diamant, Edgar Y. Choueiri, Arnold J. Kelly, and Robert G. Jahn
Electric Propulsion and Plasma Dynamics Laboratory
Princeton University, Princeton, NJ 08544

30th AIAA/ASME/SAE/ASEE Joint Propulsion Conference
June 27-29, 1994 / Indianapolis, IN

# Characterization of the Near-Anode Region of a Coaxial MPD Thruster

K. D. Diamant*, E. Y. Choueiri†, A. J. Kelly ‡, R. G. Jahn§
Electric Propulsion and Plasma Dynamics Lab
Princeton University
Princeton, New Jersey 08544



## Abstract

In an effort to identify the dominant mechanism(s) behind the creation of the anode fall, plasma potentials, temperatures, and densities along with magnetic field strengths and the electron energy distribution €unction have been measured near the anode lip of a quasisteady megawatt level MPD thruster. Temperatures, densities, and potentials recorded to within one electron Larmor radius of the anode lip along with Hall parameters based on magnetic field strengths recorded at I mm from the anode lip are presented for values of ξ (thruster current normalized by the critical ionization current} from 0.27 to 1.36. The effect of ion and electron flow velocities on probe measurements is discussed. Electron energy distribution function measurements recorded 2 mm from the anode lip for ξ values of 0.27, 0.41, and 0.44 are also presented, Above ξ = 0.44 the plasma was too noisy to permit measurements of the distribution Function. Scale lengths associated with observed variations in plasma potential indicate that magnetization of electrons is important to the establishment of the anode fall for ξ > 0.8 while for ξ < 0.8 the anode fall is a sheath phenomenon. Distribution function measurements do not show any deviation From Maxwellian behavior, indicating the absence of strong turbulence for ξ < 0.44.

## I Introduction

Energy loss to the anode significantly limits performance of magnetoplasmadynamic (MPD) thrusters. The fraction of the total thruster power deposited in the anode has been shown to be as high as 80 to 90 percent in thrusters operating at 20 kW.[1] The anode power fraction decreases with increasing thruster power, falling to 50 percent at 200kW and 10 percent at 20 MW.[2] Although anode losses are not dominant at high power, they represent a formidable problem in thermal management,

There is general agreement that electron current conduction is primarily responsible for the deposition of energy in the anode.[2-5] Electrons entering the anode deposit their enthalpy along with the work function of the anode surface and energy gained from potential differences existing near the anode surface (anodc fall). Electron enthalpy in MPD thruster plasmas typically ranges from 2.5 to 7.5 volts of effective potential, while the work functions of most anode materials are between 4 and 5 volts. In contrast, anode falls between 15 and 23 volts have been measured in a 20 kW thruster' while values from 10 to as high as 50 volts have been observed in megawatt thrusters.[6] As a result, considerable effort has gone towards identifying the physics behind the creation of the anode fall.

Classical theories regarding the production of the anode fall generally refer to a depletion of current carriers near the anode as a result of magnetic constriction.[7-10] Recently, Gallimore[11] has shown that the anode fall correlates well with the electron Hall parameter, indicating that the anode fall may be a result of electron trapping on field lines. This view is bolstered by experiments which show that the anode fall can be decreased by contouring magnetic field lines so that they intersect the anode.[5,12,13]

Non-classical theories rely on :he presence of instabilities which drive the plasma to a turbulent state in which transport properties can be strongly affected by oscillating fields. Observations of large amounts of noise (found to scale with ξ) on the operating voltage-current characteristics of MPD thrusters have prompted suspicion that turbulence exists in MRD thruster plasmas. MPDs have been shown theoretically to be susceptible to cross-field current-driven instabilities,[14,15] and it has been shown that these instabilities can significantly increase the plasma resistivity.[14] Interestingly, it was found that the magnitude of the anomalous resistivity is dependent on the Hall parameter, increasing as the Hall parameter increases.[14] The results of numerical simulation identify the anode as a region where unusually high Hall parameters are expected to exist.[16] Experimental evidence for the presence of instabilities in MPD thrusters has been obtained by Choueiri,[17] who measured the dispersion relation in a megawatt level MPD thruster and observed spatial growth of waves near the lower hybrid frequency, and by Tilley,[18] who correlated peaks in turbulence spectra measured in the exhaust plume of a 20 kW thruster with the characteristic frequencies of two current driven instabilities. Further experimental

---

* Graduate Student, Department of Mechanical and Aerospace Engineering, Member AIAA
† Research Scientist, Member AIAA
‡ Senior Research Engineer, Member AIAA
§ Professor, Department of Mechanical and Aerospace Engineering, Fellow AIAA

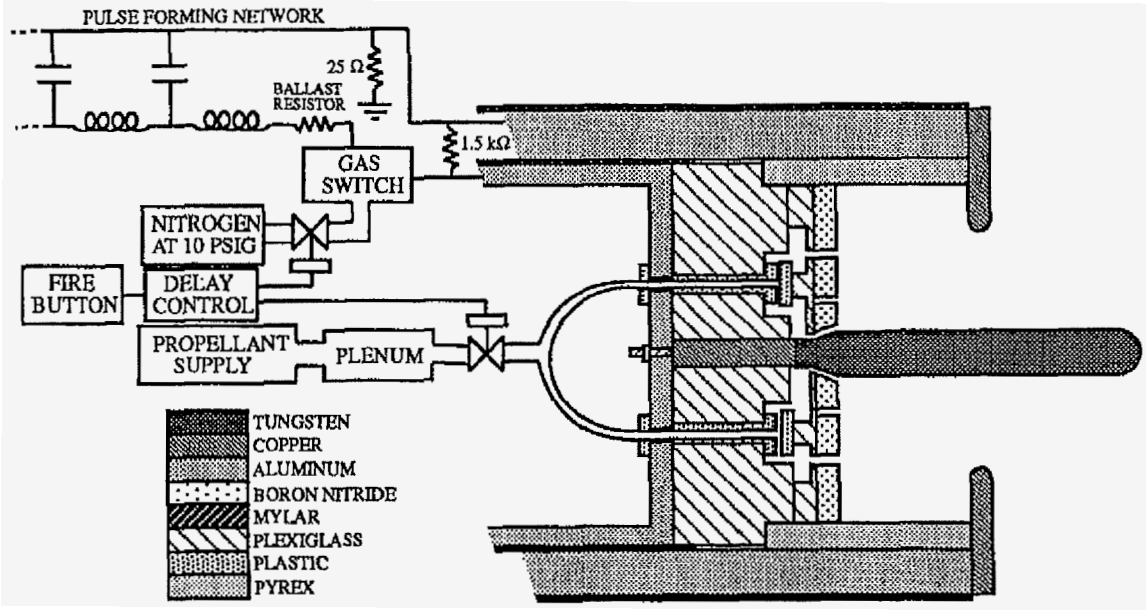


**Figure 1.** MFD Thruster.

evidence comes from Gallimore, who has inferred conductivities significantly smaller than classical values using plasma properties measured near the anode.[6] Collective effects associated with the critical ionization velocity phenomenon have also been successfully invoked to model terminal behavior[19] and rapid ionization[20] in MPD thrusters.

The goal of this study is to provide direct experimental evidence to identify the dominant mechanism for the creation of the anode fall. Each of the mechanisms described above has an associated characteristic scale length, Magnetization has the Larmor radius and a given instability will have a most unstable wavelength (the wavelength associated with maximum growth). The most unstable wavelength of the instability considered to be most likely to be present in the MPD[14,18] is approximately one order of magnitude larger than the Larmor radius. Under the assumption that each mechanism will not be operative at distances less than the mechanism's characteristic scale length from the anode, measurements of the plasma potential have been made with a resolution on the order of the Larmor radius near the anode. It is presumed that the scale length assciated with significant gradients in the plasma potential will identify the dominant effect behind the creation of the anode fall. As a supplement to this information, the electron energy distribution function has been measured near the anode in an effort to identify deviations from Maxwellian behavior that could indicate the presence of turbulence.

## II Experimental Facility

A megawatt level quasisteady pulsed MPD thruster was used in this study. The thruster is housed in a cylindrical plexiglass tank of volume 1.12 $m^3$ with an inner diameter of 0.91 m. Prior to thruster operation, the tank is maintained at a pressure of approximately 0.04 Pa ($3 \times 10^{-4}$ mm Hg) by a 15 cm oil diffusion pump and two mechanical pumps. Power is supplied to the thruster by a 160 kJ LC pulse-forming network capable of producing a rectangular current pulse of up to 52 kA for 1 msec.

The thruster consists of a cylindrical copper anode and a 2% thoriated tungsten cathode (Figure 1). The anode has an outer diameter of 19 cm, an inner diameter of 10 cm and a thickness of 1 cm , The inner radius of the anode is machined to a semi-circular lip. The cathode is 10 cm long with a 1.8 cm diameter. The thrust chamber is 5 cm deep with an inner diameter of 12.6 cm. Equal amounts of propellant are injected through twelve equispaced 3mm diameter holes at a radius of 3.8 cm in the boron nitride backplate and through an annulus around the cathode. Propellant is supplied through six sets of two sonic orifices (two sets are shown in Figure 1) and is routed to the injection holes and annulus by a plexiglass distribution plate located behind the boron nitride backplate.

Probes used in these experiments were positioned by an electrically insulated stepper motor driven positioner that is capable of providing 3 micron positioning accuracy (Figure 2). To insure that there is no relative motion between the thruster and probe during thruster operation the stepper motor is bolted to a block of

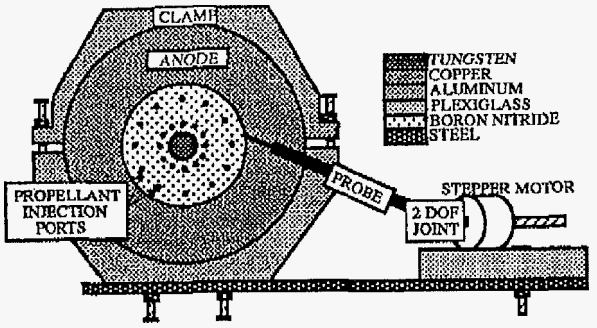


Figure 2. Robe positioned at anode lip.

plexiglass that is bolted to a 0.64 cm (0.25 inch) thick steel plate. The steel plate is bolted to two 2.5 cm (1 inch) thick aluminum clamps fastened around the body of the thruster (Figures 2 and 3). Three layers of Mylar sheet separate the clamps from the thruster body.

Probe position relative to the anode is determined with a Questar QM1 microscope-telescope attached to an Ikegami video camera (Figure 3). The system produces a multiplication factor of approximately 135 so that actual distances as small as 0.1 mm can be easily read from the video monitor.

## III Diagnostics

### III.1 Triple Probe

#### III.1.a Basic Triple Probe Theory

The triple probe is an attractive tool for measuring plasma properties because it allows the density and temperature using a steady applied voltage. Triple probes are well suited for making measurements in noisy environments where determining the slope of a ramped characteristic becomes difficult, and for situations in which plasma properties vary from run to run. One wire

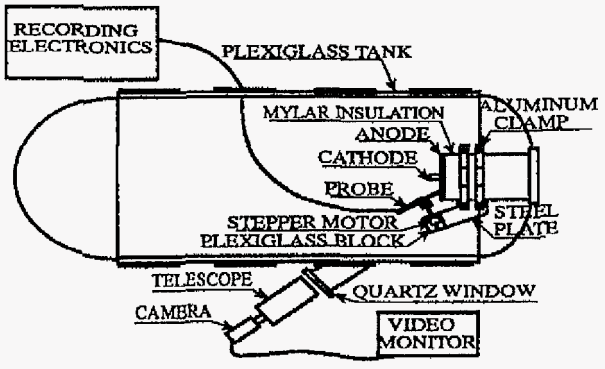


Figure 3. Top view of experiment

of a triple probe is allowed to float while the other two form a double probe with a potential difference imposed between them. When that potential difference is much larger than the temperature of the plasma then the temperature can be obtained from:

$$T(eV) = \frac{(\phi_1 - \phi_f)}{\ln\left(\frac{D_{\phi_1} + D_{\phi_2}}{D_{\phi_f}}\right)}$$

The symbol $\phi$ represents a potential with respect to plasma potential, $\phi_f$ is the floating potential and $\phi_1 - \phi_2$ is the potential difference imposed on the double probe. $D_\phi$ is the ratio of the ion current collected at potential $\phi$ to that collected at $\phi = 0$ (plasma potential) and is obtained from the numerical calculations of Laframboise for a cylindrical probe in a collisionless, quiescent plasma (or a flowing plasma in which the probe axis is aligned with the plasma flow).[21] Use of Laframboise's calculations instead of the Bohm criterion (for which $D_\phi = 1$ regardless of $\phi$) generally results in about a 10 percent improvement in accuracy. Once temperature is known, floating potentials can be converted to plasma potentials through

$$\phi_{pl} = \phi_f + T\ln\left(\frac{1}{D_{\phi_f}}\sqrt{\frac{m_i}{m_e}}\right)$$

T is the plasma temperature in eV, $m_i$ is the ion mass and $m_e$ is the electron mass. Finally, plasma density is obtained from:

$$n = \frac{I_{sat}}{D_{\phi_2} A q \sqrt{\frac{qT}{2\pi m_i}}}$$

$I_{sat}$ is the current flowing in the double probe circuit, A is the area of each double probe wire, q is the elementary charge, k is Boltzmann's constant, and again T is the plasma temperature in eV.

#### III.1.b Effect of Ion Flow

Limitations of optical access made it necessary to probe the downstream edge of the anode lip and impossible to try to orient the probe parallel to the plasma flow (Figure 4). Godard and Laframboise[22] have studied current collection by collisionless ion-attracting probes oriented transversely to an ion flow. They find that the increase in collected current resulting from the flow *is* proportionately greater for more negatively biased probes (and for probes with larger values of the ratio of probe radius to Debye length) as a result of the decreased importance of barriers in effective potential as the ion speed ratio $S_i$ ($S_i = U/(2kT_i/m_i)^{1/2}$, where U is the flow speed and $T_i$ and $m_i$ are the ion temperature and mass respectively) increases. A triple probe will record

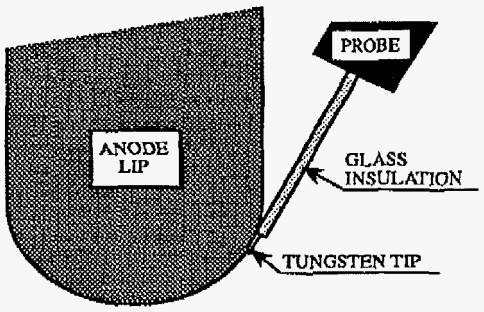


Figure 4. Orientation of probe at anode lip.

a temperature that is too high since $D_{\phi 2}$ is increased proportionately more than $D_{\phi 1}$ or $D_{\phi f}$. Floating potential readings will be too positive because of the need to attract more electrons to offset the increase in ion current (the plasma flow will not significantly increase electron current collection since flow speeds in MPD thrusters are generally an order of magnitude smaller than electron thermal velocities), and of course density measurements based on the ion saturation current will be increased. Based on the results of Godard and Laframboise[22] and a worst-case scenario for operating conditions used in this study, probe misalignment could result in temperature errors of about 10 percent, floating potential errors of about 20 percent, and densities in error by up to a factor of 3. In fact, the errors could be much larger. Tilley[23] recorded electron temperatures with a triple probe that varied by as much as 50 percent depending on probe orientation in the plume of a 20 kW MPD thruster. Tilley attributes the conservatism of Godard and Laframboise to the assumption of a symmetric sheath which may be violated in MPDs.

Fortunately for this study the proximity of the probe to the anode may reduce the effect of ion flow since the probe may lie within a boundary layer, The momentum diffusivity for a gas is approximately equal to the product of a mean free path and a thermal velocity. For ions in the plasma near the anode this product is on the order of one. An effective boundary layer depth might then be:

$$\lambda_{bl} = [\text{width of anode lip/plasma flow velocity}]^{1/2}$$

The width of the anode lip is $10^{-2}$ m while the plasma flow velocity, based on the $bJ^2$ thrust law[24] for conditions used in this study, is approximately $10^3$ to $10^4$ m/s yielding $\lambda_{bl}$ = 1 to 3 mm. Since the ion thermal velocity is also expected to be between $10^3$ and $10^4$ m/s thermal effects may be expected to dominate within 1 mm of the anode.

### III.1.c Effect of Electron Drift

Electron drifts in an MPD thruster which could potentially affect probe measurements are those associated with current conduction and with electrons free-falling through potential differences that exist over scale lengths smaller than one electron-ion mean free path, Electron thermal velocities for most operating conditions are $O(10^5)$ m/s. Measurements of electron number and current density[4] indicate that electron current velocities near the anode can be as large as $5 \cdot 10^4$ m/s. More significantly, in this study electron-attracting potential drops up to three times the magnitude of the electron temperature are measured over scale lengths much smaller than an electron-ion mean free path at distances on the order of the electron Larmor radius from the anode lip. Assuming these measurements to be accurate leads to the conclusion that the potential exists for the electrons to develop a drift velocity in excess of their thermal velocity.

The problem of electron current collected by a negatively biased probe oriented transversely to a collisionless flowing plasma has been treated by Kanal[25] and Hoegy and Wharton.[26] Kanal presents the following expression for the ratio of the current collected by a probe in a flowing plasma to that for the case of no flow (the symbol $B_v$ will be used to represent this ratio):

$$B_v = e^{-S_e^2} \sum_{n=0}^{\infty} \frac{(2n+1)!S_e^n}{(n!)^2 2^{2n} (V)^{n/2}} I_n[2S_e V^{1/2}]$$

$S_e$ is the electron speed ratio $(U/(2kT_e/m_e)^{1/2})$, V is the probe potential with respect to the plasma normalized by the electron temperature in eV (V is to be taken as positive in this expression), and $I_n$ is the modified Bessel function of order n. Hoegy and Wharton claim that Kanal's expression is valid only for small values of $S_e$ and suggest the following expression as valid for $S_e$ on the order of $V^{1/2}$:

$$B_v = \frac{e^V \sqrt{S_e}}{2} \sum_{n,p=0}^{N,P} \left(\frac{\varepsilon / S_e}{n!}\right)^n \left(\frac{1/S_e}{p!}\right)^p G$$

G is a ratio of gamma functions given by:

$$G = \frac{\Gamma\left(\frac{5}{4} + \frac{1}{2}(p-n)\right)}{\left[\Gamma\left(\frac{5}{4} - \frac{1}{2}(p+n)\right)\right]^2}$$

and $\varepsilon = S_e^2 - V$. A plot of both expressions as a function of potential drop experienced by the electrons normalized by the electron temperature (effectively $S_e^2$) for a few values of V (Figure 5) shows that Hoegy and

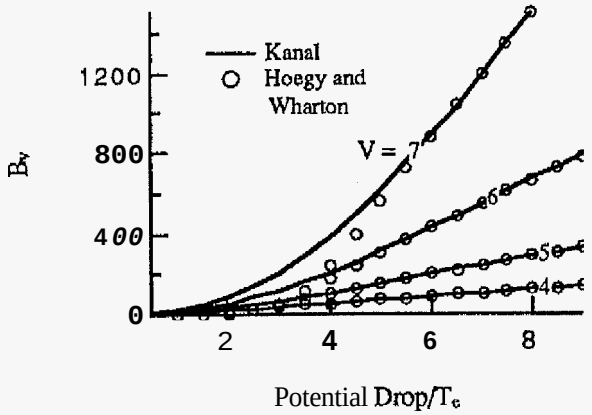


Figure 5. Comparison of Kanal and Hoegy and Wharton

Wharton are in complete agreement with Kanal in the region where Hoegy and Wharton claim their expression to be valid. Since Kanal's result appears to be valid over a wider range of $S_n$ it will be used for this study.

In the case of an electron drift the expressions for plasma potential and temperature presented in section I.a. are modified to read:

$$\phi_{pl} = \phi_f + T\ln\left(\sqrt{\frac{m_i}{m_e}}\frac{B_{v_f}}{D_{\phi_f}}\right)$$

$$T(eV) = \frac{(\phi_1 - \phi_f)}{\ln\left(\frac{D_{\phi_1} + D_{\phi_2}}{D_{\phi_f}}\frac{B_{v_f}}{B_{v_1}}\right)}$$

$B_{vf}$ and $B_{v1}$ represent Kanal's ratio for a probe at potential $\phi_f$ (floating potential) and $\phi_1$ respectively. Figure 5 shows that the increase in the current collected is proportionately greater for probes that are biased more negatively. $B_{vf}$ will be greater than $B_{v1}$ and the probe will indicate a temperature that is too high. This error turns out not to be severe and is relatively insensitive to the size of the potential drop that creates the drift. For potential drops of 1, 2, and 3 times the electron temperature, it is found that the error incurred in the temperature measurement as a result of ignoring the electron drift is approximately 30 percent.

Floating potential measurements can be severely impacted by drift. This is to be expected since ion collection is extremely insensitive to changes in potential below the actual plasma floating potential (the probe radius to Debye length ratio for the probe used in this study is approximately 30). This means that the excess negative potential assumed by the probe in order to float is directed almost entirely at repelling the oncoming electrons since only a small increase in ion collection will be realized. In the case of no drift, the difference between floating and plasma potentials, normalized by the electron temperature is about five. For drift-creating potential drops of 1, 2, and 3 times the electron temperature, this number increases from 5 to 9, 11, and 14 respectively. If there actually was an electron-attracting potential change of twice the electron temperature, the triple probe would indicate an electron-repelling potential change of four times the electron temperature. The impact of electron drift on the measurements presented here will be discussed in the results section.

It should be noted that both Kanal, and Hoegy and Wharton assume a symmetric sheath in their calculations. This assumption is expected to break down at large speed ratios and it is uncertain how this could affect the conclusions presented above.

### III.1.d Probe Construction

For these experiments it was necessary to construct a triple probe with a resolution of 0.1 mm. Three 0.064 mm (2.5 mil) diameter tungsten wires were individually coated with glass by threading each wire through a glass tube, heating the tube with a propane torch, and then drawing the glass down to the wire. A fourth tube was then heated and drawn over the three wires to hold them in place. The small size and delicate nature of the probe made it impossible to mechanically trim the tip. so acids were used to remove unwanted material. Hydrofluoric acid was used to dissolve glass while a half-and-half mixture of hydrofluoric and nitric acids was used to trim the tungsten. Pans of the probe that were not to be etched were protected from the acid and acid vapor by covering them with candle wax. The wax was applied and removed with a heat gun, The finished probe has a tip length of 0.94 mm with a separation between adjacent wires of about one wire radius. The wires are in a line so that they will all be the same distance from the anode (when viewed from the side the probe appears to have only one wire at the tip). A tip length of 0.94mm results in an error in the probe position relative to the anode due to anode lip curvature that is approximately the same as the error associated with the finite radius of the probe wires.

### III.2 Magnetic Probe

Knowledge of the magnetic field near the anode is required to make estimates of the electon Larmor radius and Hall parameter. A magnetic induction probe with a resolution of 1 mm was constructed by wrapping 40 turns of 0.046 mm (1.8 mil) copper magnet wire around a 0.87 mm diameter alumina core. The coil is protected from the discharge by a rectangular glass sleeve with an exterior width of 2 mm. The sleeve was made by extruding a rectangular strip of brass into a heated glass tube so that the glass molded around the strip. The brass

was removed with nitric acid. Calibration was performed with a Helmholtz coil supplied with a rectangular current pulse. Hoskins[27] describes the high-gain integrator needed to make these measurements.

### III.3 Electron Distribution Function

Measurement of the electron distribution function is necessary to assess deviations from Maxwellian behavior that may be the result of the influence of plasma instabilities. The distribution function can be obtained by double differentiation of the expression for electron current collected by a non-concave electron retarding probe[28]:

$$f(eV) = \frac{2\sqrt{2}}{Aq^2}\sqrt{\frac{m\phi}{q}}\frac{d^2 I_e}{d\phi^2}$$

f is the electron energy distribution function, A is the probe area, q is the elementary charge, m is the electron mass, $\phi$ is the probe potential with respect to the plasma, and $I_e$ is the electron current collected at $\phi$.

Knowledge of the electron current characteristic ($I_e$ vs $\phi$) is required, however Langmuir probes measure the total (ion plus electron) current-voltage characteristic. For voltages less than about 5 times (for argon) the electron temperature below plasma potential electron current dominates ion current and the total current voltage characteristic can be considered equal to the electron characteristic. At greater voltage differences it can be shown that while the ion current exceeds the electron current, the curvature of the ion current is negligible in relation to that of the electrons. If the electrons have a Maxwellian distribution, then the curvature of the electron current is given by:

$$\frac{d^2 I_e}{d\phi^2} = \frac{I_e}{T^2} e^{-\frac{e}{T}}$$

$I_e$ is the electron current collected at $\phi = 0$ and T is the electron temperature in eV. Peterson and Talbot[29] have determined algebraic fits to the numerical calculations of Laframboise[21] concerning the ion current collected by an ion attracting cylindrical probe. For the case of equal ion and electron temperatures and for a probe of radius equal to about 30 Debye lengths they claim that the following expression fits Laframboise's calculations to within 3 percent for $|\phi/T| > 3$:

$$I_i = I_{oi}\left(7.7 + \left|\frac{\phi}{T}\right|\right)^{0.24}$$

$I_i$ is the ion current collected at $\phi = 0$. Using these two expressions it can be shown that for voltages less than 10 times the electron temperature below plasma potential the curvature of the total Langmuir probe current characteristic can be equated to that of the electron current with an error of 10 percent or less (at a voltage of 8 times the electron temperature the error is 1 percent).

The simplest methods available for determining the curvature of the probe characteristic are to digitally record and numerically differentiate it, or to feed the probe output into differentiating electronics. Both of these methods are suitable only for extremely quiescent plasmas, For noisy plasmas a third method first used by Sloane and MacGregor[30] is available which involves superimposing a small amplitude alternating potential on the steady probe bias. The second derivative is obtained from the amplitude of the probe current at the imposed modulation frequency or a harmonic of that frequency, depending on the form of the imposed alternating potential.[31] Sloane and MacGregor[30] actually obtained the second derivative from an increase in the dc current level, but that approach was adopted probably because of a lack of narrow bandwidth detector technology at the time. The method is described as follows.[28]

The relationship between probe current and potential can be written as:

$$I = I(\phi)$$

If a small oscillating potential v is added to the steady probe bias $\phi$ then it is possible to describe the resulting current using a Taylor expansion about the value of the current at $\phi$:

$$I(\phi + v) = I(\phi) + v\frac{dI}{d\phi} + \frac{v^2}{2}\frac{d^2 I}{d\phi^2} + \cdots$$

The above statement should be valid for any value of v since $I(\phi)$ is likely to have an exponential form (for Maxwellian plasma) and the Taylor series of $e^x$ converges for all x. The simplest choice for v is a pure sine wave at frequency w with amplitude $v_o$:

$$v = v_o \sin\omega t$$

In that case the probe current is given by:

$$I = I(\phi) + v_o \sin\omega t\frac{dI}{d\phi} + \frac{v_o^2}{4}(1 - \cos 2\omega t)\frac{d^2 I}{d\phi^2} + \cdots$$

The amplitude of the current at frequency $2\omega$ is then proportional to the second derivative of the current at potential $\phi$. If the Taylor series is written out to include higher order terms it is found that components at frequency $2\omega$ appear in front of all the even derivatives of I. Contributions from the fourth, sixth, eighth, and tench derivatives are:

$$\frac{v_o^4}{48}I^{(4)} - \frac{v_o^6}{1536}I^{(6)} - \frac{v_o^8}{92160}I^{(8)} - \frac{v_o^{10}}{8.8\cdot 10^6}I^{(10)}$$

$I^{(n)}$ represents the nth derivative of I with respect to $\phi$. The above result was obtained from a symbolic manipulation program called MAPLE. The first two terms shown are corroborated by Branner, et al.[30] If the amplitude $v_o$ is taken to be 1 volt then the error associated with assuming that the amplitude at frequency

$2\omega$ comes safely from the $v_o^2$ term is about 2 percent for a plasma with a temperature of 2 eV (assuming Maxwellian electrons, each successive derivative of the current is smaller by a factor of 1/T(eV) than its predecessor). The higher order terms are included to show how rapidly the series decreases.

A single Langmuir probe was placed 2 mm from the anode lip, and a dc bias summed with a 1 volt amplitude, 50 kHz sine wave was applied to it. Because of current drive capability limitations of the electronics producing the probe signal, a 0.01 mm diameter probe with a tip length of 0.49 mm was used to record the low energy end of the distribution while a 0.064 mm (2.5 mil) diameter probe with a tip length of 0.42 mm was used to record the high energy end, A frequency of 50 kHz was chosen because it differs significantly from the base frequency of the rectangular thruster pulse (1 kHz) and is at least an order of magnitude away from any natural plasma frequencies. The voltage drop across a 1 Ω resistor in series with the probe provided a measure of the probe current, and this signal was fed to an EG&G Instruments model 5210 lock-in amplifier tuned to 100 kHz. Because of the short duration of the thruster pulse (1 millisecond), the output time constant of the lock-in amplifier was set to 100 microseconds, resulting in an output bandwidth of approximately 1 kHz.

The primary source of error in the distribution function measurements presented here is the uncertainty in the value of the plasma potential, particularly at the low energy end of the distribution where the difference between the probe potential and plasma potential is small. These experiments were conducted with a copper anode, and it has been observed that during firings the surface of the anode darkens and as it does so the plasma potential near the anode becomes more negative. Differences of several volts are commonly observed during the course of as few as 20 firings. The anode can be "reset" by sanding off the darkened surface layer. It is possible that the darkening of the surface results from a reaction between the copper and diffusion pump oil present io the tank. To compensate for this problem, measurements of the plasma floating potential were made after every three firings. These measurements were converted to plasma potentials using triple probe temperature measurements and standard probe theory which assumes a Maxwellian plasma. In the future this experiment will be conducted with an aluminum anode in an attempt to maintain a more stable value of the plasma potential. Also, due to the current drive limitations of the equipment used to produce the probe signal, the low energy data had to be taken with a very small probe (0.01 mm diameter tungsten wire). This probe has a non-negligible resistance (51 ohms) and it was necessary to correct for reductions in the amplitude of the ac signal (and of course the dc bias) being sent to the probe due to its collected current. This correction is obtained by estimating the amplitude of the current collected at the input frequency w from knowledge of the first derivative of the collected current (see expression for $I(\phi + v)$ above). The first derivative of the collected current is in turn estimated by assuming a Maxwellian plasma and making use of triple probe temperature measurements along with collected currents measured with the 0.01 mm diameter probe. Percentage errors associated with this correction are generally less than half the size of those associated with the determination of the difference between the probe and plasma potentials.

## IV Results

### IV.1 Plasma Processes Near the Anode Lip

Plasma potentials, temperatures, and densities as well as magnetic field strengths have been measured near the anode lip for values of $\xi$ ranging from 0.27 to 1.36 with argon as propellant (Figures 6 to 8). $\xi$ is defined as the ratio of the thruster current to the critical ionization current, and has been identified as an important scaling parameter in MPD thruster operation.[19] For clarity, on each plot only one vertical error bar is shown for each operating condition. The percentage emf represented by that error bar is the same for all points in the same operating condition, Error bars for the probe position relative to the anode are the same for all operating conditions and are shown for one operating condition on each plot.

Figure 6 shows the variation of plasma potential normalized by the thruster operating voltage. All plasma potentials are negative with respect to the anode. Estimates of the electron Larmor radius based on temperatures recorded at 0.1 mm from the anode and magnetic fields recorded at 1 mm from the anode are shown in the legends of those plots.

There is a change in behavior that occurs at approximately $\xi = 0.8$, For $\xi$ values above 0.8 the only significant feature is a consistent positive increase in the plasma potential that occurs within 0.5 mm of the anode. In almost all cases the magnitude of these increases is less than the size of the error bars associated with the measurements. but the consistency of the increases makes them difficult to dismiss. Choueiri has shown that the most unstable wavlength associated with the instability considered most likely to be present in MPD thrusters is approximately 16 times the size of the electron Larmor radius (Choueiri finds $kr_L = 0.4$ where k is the most unstable wavenumber).[14] The characteristic scale length for the observed changes in plasma potential appears however to be on the order of the Larmor radius itself, indicating that magnetization of electrons is more likely to be influencing the anode fall than is turbulence. A further indication of the importance of magnetization for $\xi$ values greater than 0.8 is the appearance of very large values of the Hall parameter near the anode (Figure 9a).

The results of section III.1.c indicate that if electrons were actually free-falling through the potential differences shown in Figure 6a then it should not be possible to measure those differences. In fact the discussion of section III.1.c is probably not entirely applicable to the data in Figure 6a because of the large Hall parameters observed at those conditions. In the case of the Hall parameter being much larger than one, the scale length for diffusing electrons becomes the Larmor radius instead of the mean free path[32] (electron-ion mean free paths are on the order of 1 mm). It is likely then that at least one thermalizing collision will occur as the electrons traverse those potential differences.

For $\xi$ values less than 0.8 (Figure 6b) there is again very little variation in the plasma potential up to about 0.5 mm from the anode lip. Inside 0.5 mm there is a small, consistently measured negative increase in the plasma potential. The Larmor radii are slightly larger at these lower currents, and it is possible that these negative increases are artificial, created by drifting electrons. Use of Kanal's theory predicts that the size of an electron attracting potential drop required to create the measured electron repelling increases is only about 0.2 times the electron temperatue. We are of the opinion that for $\xi$ values less than 0.8 the anode fall is occuring in a sheath (scaled by the Debye length). The diminished importance of magnetization is evident from Figure 9b in which the Hall parameter does not exceed eight,

A qualitative argument can be made to reinforce the conclusions drawn above. Figure 8 shows the variation in plasma density approaching the anode. The density is observed to drop fairly rapidly inside of 1 mm from the anode. If it is assumed that this drop is not entirely due to the probe entering the anode boundary layer and that current density remains relatively constant, then the drop in density must be accompanied by an increase in current velocity. The energy for this increase has to come either from thermal energy or from a decrease in potential energy. For $\xi < 0.8$, Figure 7b shows smoothly decreasing temperatures inside of 1 mm that are of a magnitude appropriate for maintaining constant current density. It could be argued then that electron attracting potential changes would be energetically unnecessary in that region. In contrast, temperatures recorded for $\xi <$ 0.8 do not show a regular decrease inside of 1 mm, thus creating a need for electron attracting potential drops to maintain current density.

The discussion in the previous paragraph again brings up the question of the effect of electron drift on the probe data. Density measurements indicate that if current density remains constant then current velocities must increase by more than a factor of two in most cases as the anode is approached. Current velocities would then be of the same order of magnitude as the electron thermal velocity, and the results of section III.1.c indicate that measured potentials should be strongly shifted toward more electron repelling values. Since strong shifts are not observed, it is conjectured that the large Hall parameters new the anode are forcing this increased current velocity to flow along the anode and hence along the axis of the probe (rather than perpendicular to the probe).

### IV.2 Distribution Function

The electron energy distribution function was measured at a distance of 2 mm from the anode lip for $\xi$ values of 0.27, 0.41, and 0.44 €or argon mass flaw rates of 16, 16, and 6 g/s respectively (Figures 10 to 12). Attempts to obtain measurements at $\xi$ values greater than 0.44 were unsuccesful due to large amounts of noise present in the discharge. It is suspected that use of an aluminum anode instead of the current copper anode may reduce this noise and allow measurements at higher $\xi$ values.[33] The dashed curves shown on each plot are the upper and lower limits of a Maxwellian distribution based on triple probe measurements of density and temperature and the errors associated with those measurements. It is found that, to within the range specified by the error bars, the data lies within the band defined by the Maxwellians.

The exact manner in which the distribution function should be affected by turbulence is not well known at this point. However, it is our opinion that the lack of significant deviation from Maxwellian behavior can be taken as an indication of the absence of strong turbulence near the anode for the given $\xi$ values.

## V. Conclusion

In an attempt to identify the dominant mechanism behind the creation of the anode fall, electrostatic and magnetic probes were used to characterize the plasma near the anode lip of a quasisteady megawatt level MPD thruster for values of $\xi$ ranging from 0.27 to 1.36. Profiles of plasma potential show that significant changes toward more positive potentials were observed to occur only within a distance from the anode comparable to the electron Larmor radius for $\xi > 0.8$. For $\xi < 0.8$ small negative changes in the plasma potential were observed in the same region, but it is believed that these are the artificial result of electron drifts. No significant variations in plasma potential were observed over scale lengths comparable to the most unstable wavlength of plasma turbulence predicted to be present. Measurements of the electron energy distribution function for $\xi$ values of 0.27, 0.41, and 0.44 do not show any deviation from Maxwellian behavior, which is taken as an indication of the absence of strong turbulence, even though the exact influence that turbulence would have on the distribution function is not well known. The evidence indicates that magnetization of electrons is important in the establishment of the anode fall for $\xi > 0.8$ while for $\xi < 0.8$ sheath effects are likely to dominate.

## Acknowledgements

The authors wish to thank George E. Miller for his invaluable assistance *in* the laboratory, *and* EG&G Instruments for their generosity and technical support. This work is supported by the Fannie and John Hertz Foundation and by the National Aeronautics and Space Administration under contract # 954997.

## References

1. Myers, R. M., "Energy Deposition in Low Power Coaxial Plasma Thrusters", Ph.D. Thesis, Princeton University, June 1989.

2. Saber, A. J., "Anode Power in a Quasi-Steady MPD Thruster", Ph.D. Thesis, Princeton University, 1974.

3. Oberth, R. C., "Anode Phenomena in High-Current Accelerators", AIAA 71-198, AIAA 9th Aerospace Sciences Meeting, New York, New York, Jan. 1971.

4. Gallimore, A. D., Kelly, A. J., and Jahn, R. G., "Anode Power Deposition in Quasi-Steady MPD Thrusters", AIAA 90-2668, 21st International Electric Propulsion Conference, Orlando, Florida, July 1990.

5. Soulas, G. C., Myers, R. M., "Mechanisms of Anode Power Deposition in a Low Pressure Free Burning Arc", NASA Contractor Report 194442, IEPC 93-194.

6. Gallimore, A, D., Kelly, A. J., and Jahn, R. G., "Anode Power Deposition in MPD Thrusters", IEPC 91-125, 22nd International Electric Propulsion Conference. Viareggio, Italy, October 1991.

7. Hugel, H., "Effect of Self-Magnetic Forces on the Anode Mechanism of a High Current Discharge", IEEE Transactions on Plasma Science, Vol. PS-8, No. 4, December 1980, pp. 437-442.

8. Korsun, A. G., "Current Limiting by Self Magnetic Field in a Plasma Accelerator", Soviet Physics Technical Physics, Vol. 19, No. 1, July 1974.

9, Vainberg, L. I., Lyubimov, G. A., and Smolin, G. G., "High-Current Discharge Effects and Anode Damage in an End-Fire Plasma Accelerator", Soviet Physics Technical Physics, Vol. 23, No. 4, April 1978.

10. Baksht, F. G., Moizhes, B. Ya., and Rybakov, A, B., "Critical Regime of a Plasma Accelerator", Soviet Physics Technical Physics, Vol. 18, No. 12, June 1974.

11. Gallimore, A. D., "Anode Power Deposition in Coaxial MPD Thrusters", Ph.D. Thesis, Princeton University, October 1992.

12. Schall, W., "Influence of Magnetic Fields on Anode Losses in MPD Arcs", AIAA 72-502, AIAA 9th Electric Propulsion Conference, Bethesda, MD., April 1972.

13. Schcuer, 3. T., Hoyt, R. P., Schoenberg, K. F., Gerwin, R. A., Moses, R. W., and Henins, I., "Control and Minimization of Anode Fall in a Quasisteady Nozzle-Based Coaxial Plasma Thruster", IEPC 93-118, 23rd International Electric Propulsion Conference, Seattle, Washington, September 1993.

14. Choueiri, E. Y., "Electron-Ion Streaming Instabilities of an Electromagnetically Accelerated Plasma", Ph.D. Thesis, Princeton University, 1991.

15. Aref'ev, V. I., "Current-Driven Instabilities in a Strongly Inhomogeneous Plamsa. I", Soviet Physics Technical Physics, Vol. 17, No. 7, January 1973.

16. Caldo, G., Choueiri, E. Y., Kelly, A. J., Jahn, R. G., "An MPD Code with Anomalous Transport". IEPC 91-102, 22nd International Electric Propulsion Conference, Viareggio, Italy, October 1991.

17. Choueiri, E. Y., Kelly, A. J., Jahn, R. G., "Current-Driven Plasma Acceleration Versus Current-Driven Energy Dissipation, Part II: Electromagnetic Wave Stability Theory and Experiments", IEPC 91-100, 22nd International Electric Propulsion Conference, Viareggio, Italy, October, 1991.

18. Tilley, D. L., Choueiri, E. Y., Kelly, A. J., Jahn, R. G., "An Investigation of Microinstabilities in a kW Level Self-Field MPD Thruster", IEPC 91-122, 22nd International Electric Propulsion Conference, Viareggio, Italy, October 1991.

19. Choueiri, E. Y., Kelly, A. J., Jahn, R. G., "MPD Thruster Instability Studies", AIAA 87-1067, 19th International Electric Propulsion Conference, Colorado Springs, Colorado, 1987

20. Choueiri, E. Y., Okuda, H., "Anomalous Ionization in the MPD Thruster", IEPC 93-067, 23rd International Electric Propulsion Conference, Seattle, WA., September 1993.

21. Laframboise, J. G., "Theory of Spherical and Cylindrical Langmuir Probes in a Collisionless, Maxwellian Plasma at Rest", Rept. 100, University of Toronto Institute for Aerospace Studies, 1966.

22. Godard, R., Laframboise, J. G., 'Total Current to Cylindrical Collectors in Collisionless Plasma Flow", Planet. Space Sci., Val. 31, No. 3, pp. 275-283, 1983.

23. Tilley, D. L., Kelly, A. J., and Jahn, R. G., "The Application of the Triple Probe Method to MPD Thruster Plumes", AIAA 90-2667, 21st International Electric Propulsion Conference, Orlando, Florida, July 1990.

24, Jahn, R. G., The Physics of Electric Propulsion, McGraw Hill, 1968, pp. 240-246.

25. Kanal, M., "Theory of Current Collection of Moving Cylindrical Probes", Journal of Applied Physics, Vol. 35, No. 6, June 1964.

26. Hoegy, W. R. and Wharton, L. E., "Current to a Moving Cylindrical Electrostatic Probe", Journal of Applied Physics, Vol. 44, No. 12, December 1973.

27. Hoskins, W. A., "Asymmetric Discharge Patterns in the MPD Thruster", M.S. Thesis, Princeton University, 1990.

28. Swift, J. D. and Schwar, M. J. R., Electrical Probes for Plasma Diagnostics, American Elsevier Publishing Company, Inc. New York, New York, 1970.

29. Peterson, E. W. and Talbot, L., "Collisionless Electrostatic Single-Probe and Double-Probe Measurements", AIAA Journal, Vol. 8, No. 12, December 1970, pp. 2215-2219.

30. Sloane, R. H. and MacGregor, E. I. R., "An A.C. Method for Collector Analysis of Discharge Tubes", Phil. Mag, 7th Series, No, 117, 1934.

31. Branner, G. R., Friar, E. M. and Medicus, G.. "Automatic Plotting Device for the Second Derivative of Langmuir Probe Curves", Rev. Sci. Instrum., Vol. 34, 1963, pp. 231-237.

32. Chen, F. F. Introduction to Plasma Physics and Controlled Fusion, 2nd Ed., Plenum Press, New York, 1984.

33. Gallimore, A. D., Personal Communication.

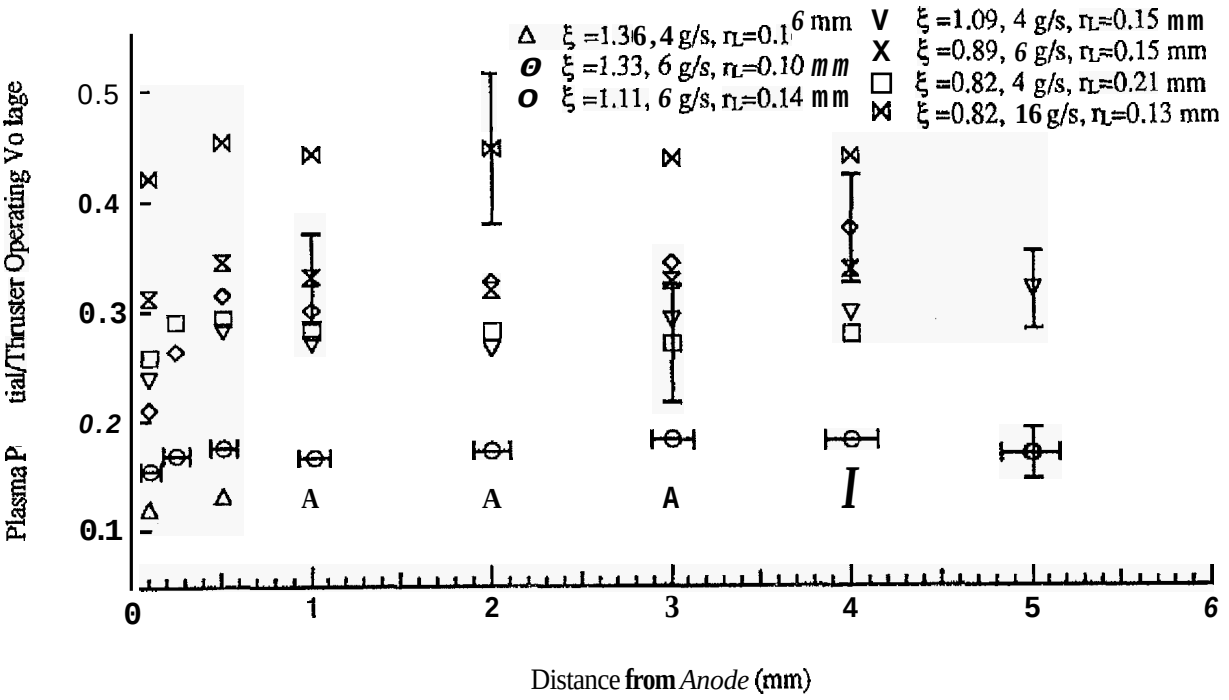


Figure 6a. Plasma potentials for $\xi$ = 1.36 to 0.82.

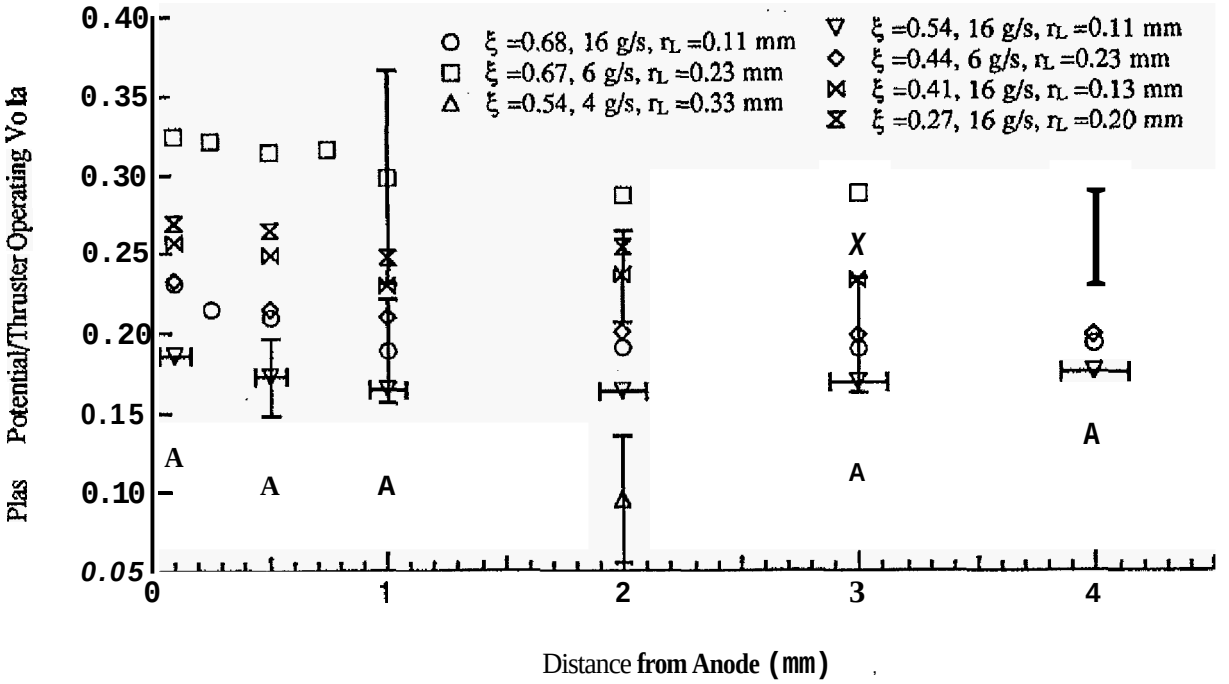


Figure 6b. Plasma potentials $\xi$ = 0.68 to 0.27.

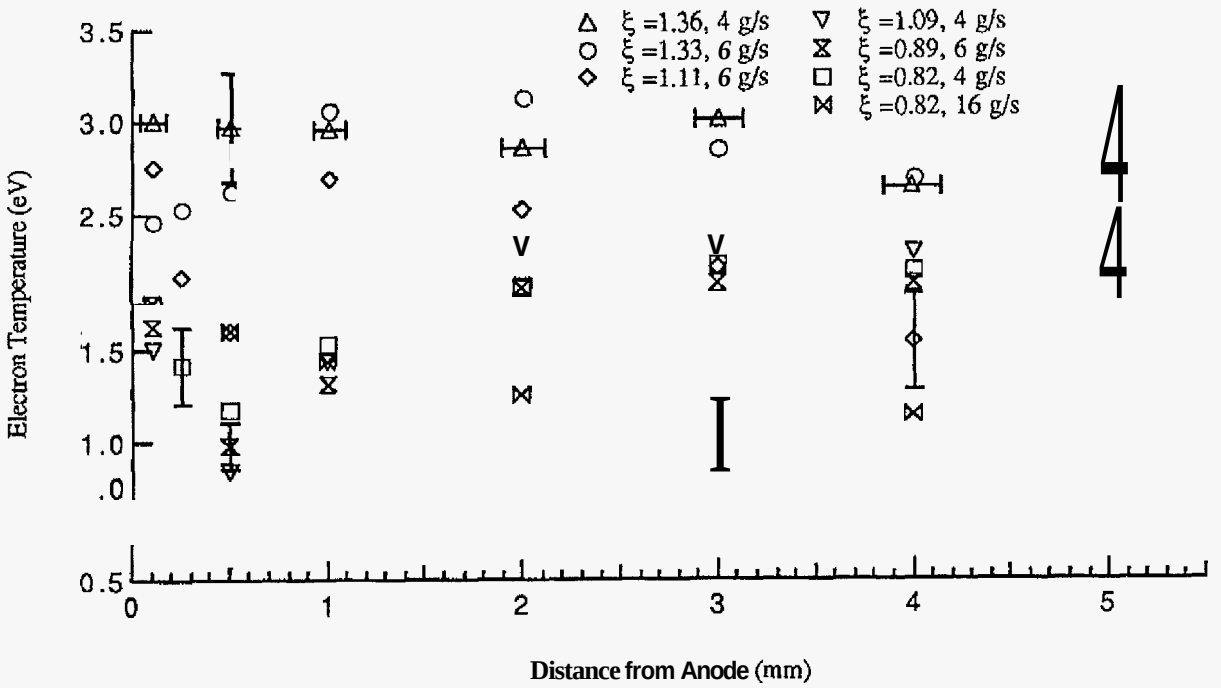


Figure 7a. Electron **temperatures for** $\xi$ = **1.36** *to* 0.82.

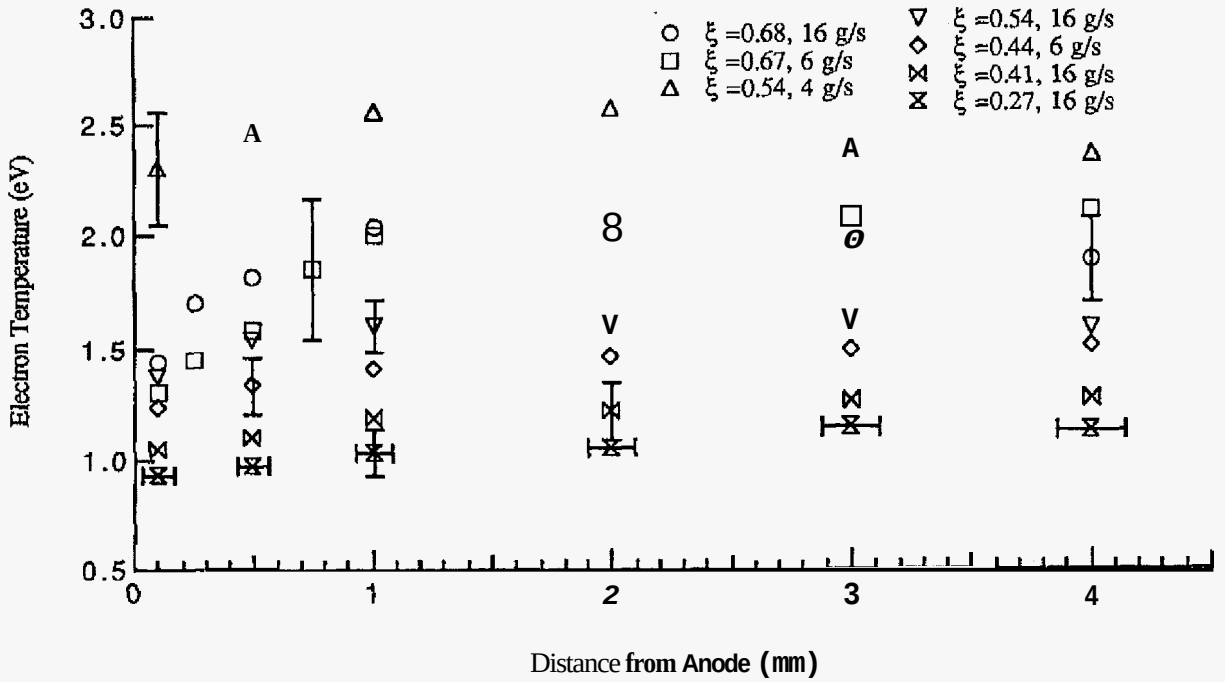


**Figure 7b. Electron** temperatures **for** $\xi$ = 0.68 *to* 0.27,

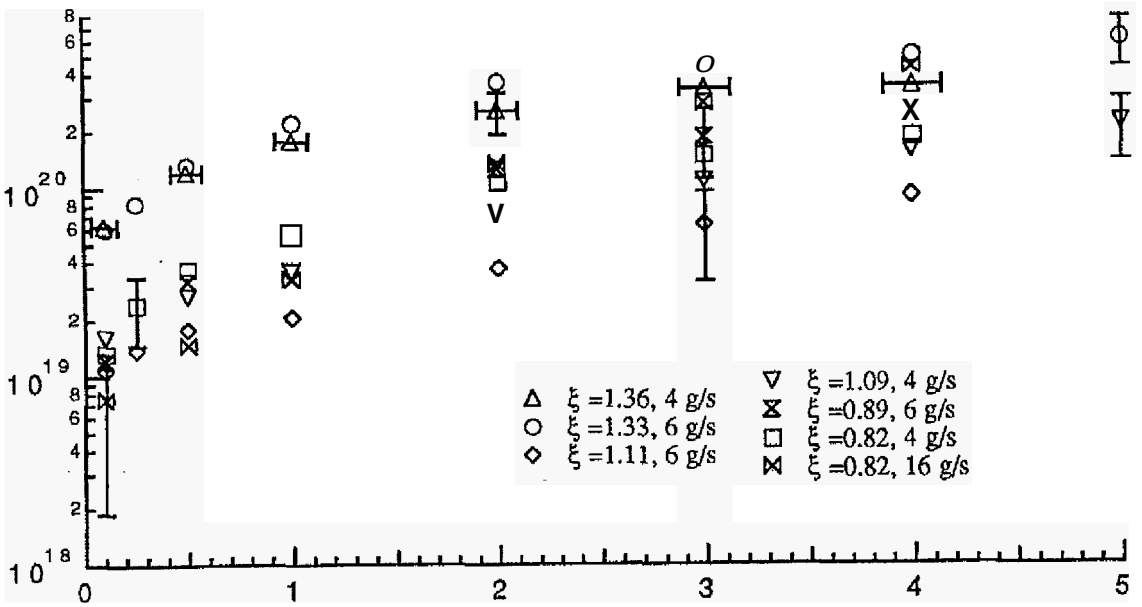


Figure 8a. Plasma density for $\xi$ = 1.36 to 0.82.

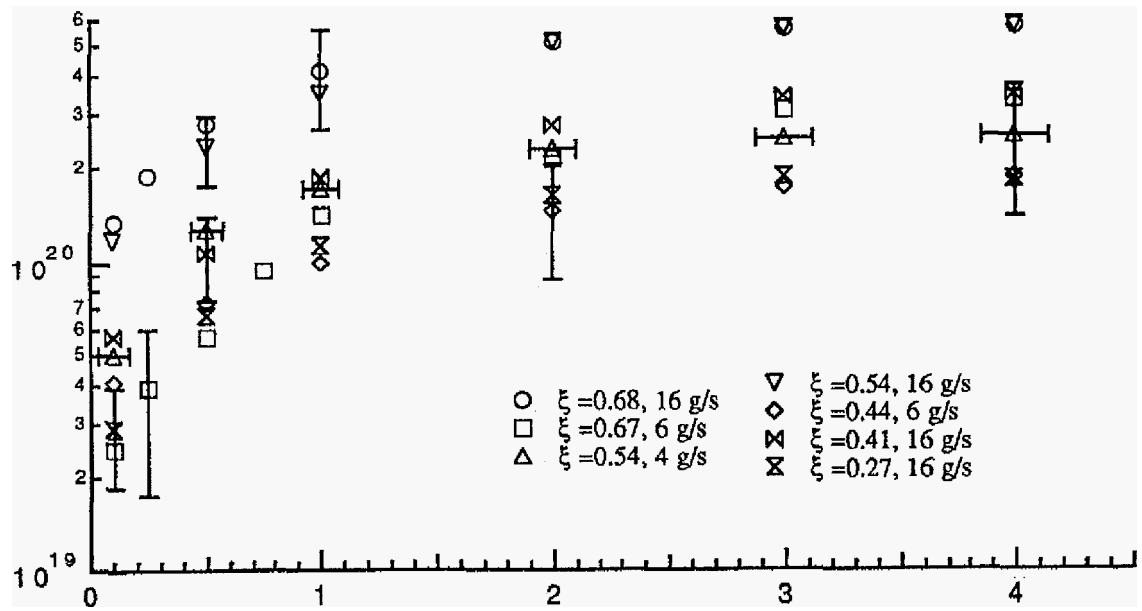


Figure 8b. Plasma density for $\xi$ = 0.68 to 0.27.

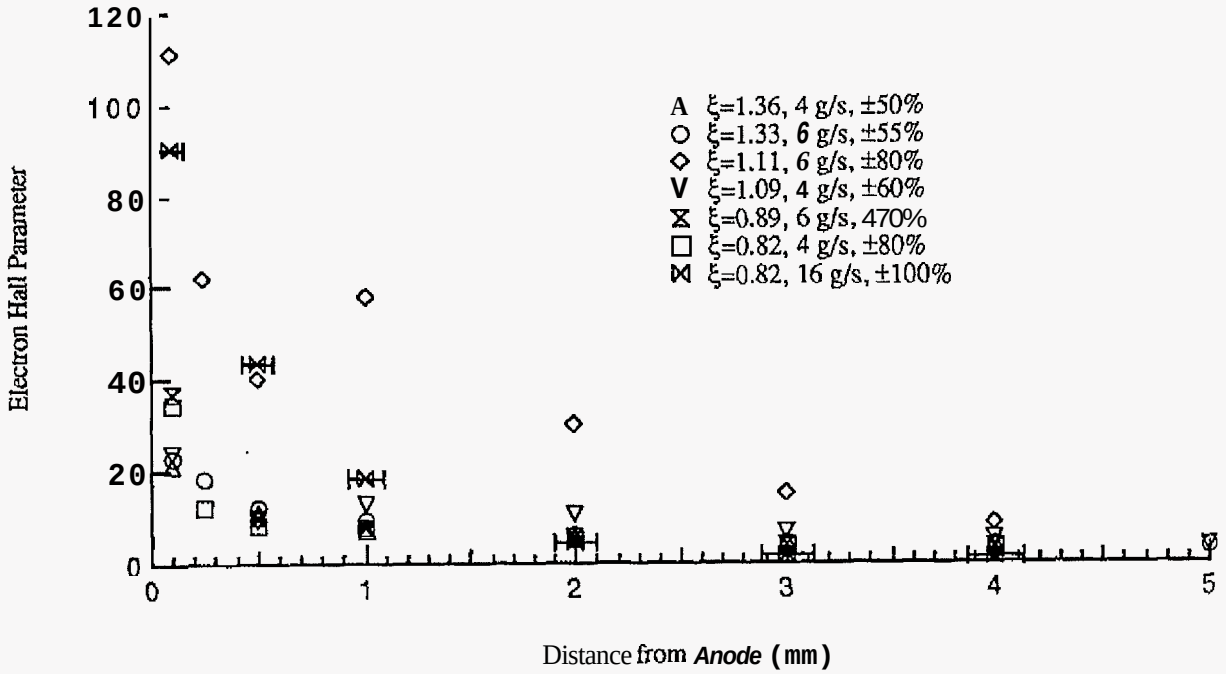


**Figure 9a. Electron Hall parameter for ξ = 1.36 to 0.82.**

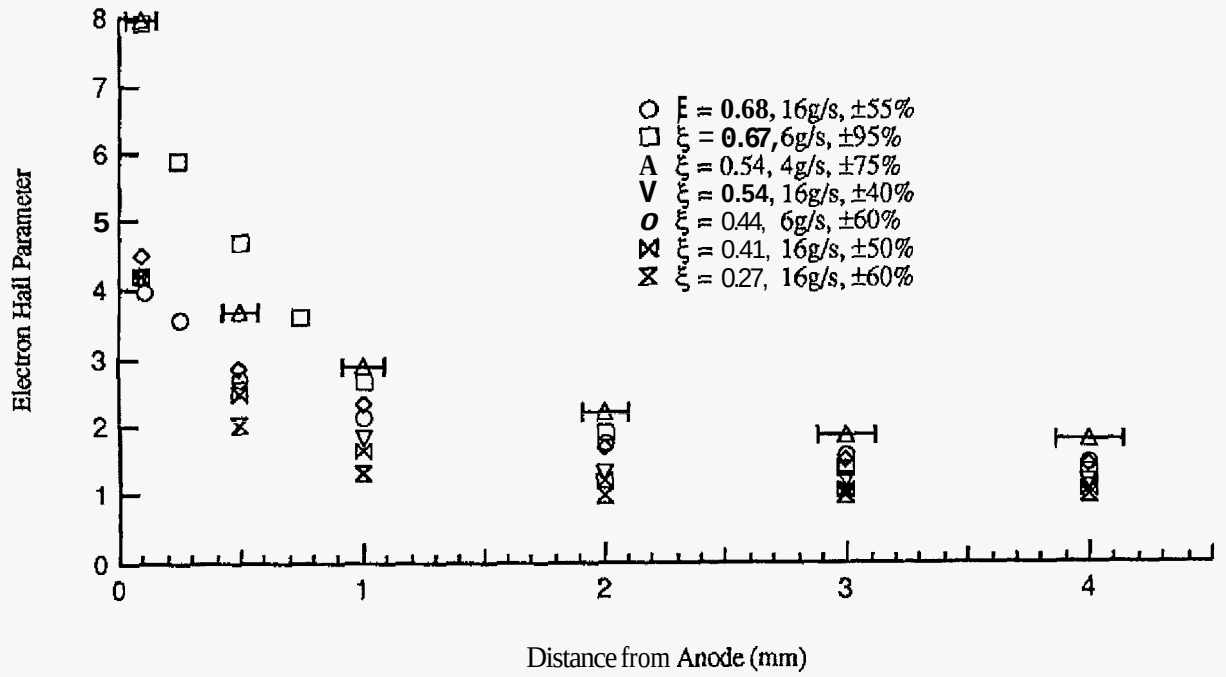


**Figure 9b. Electron Hall parameter for ξ = 0.68 to 0.27,**

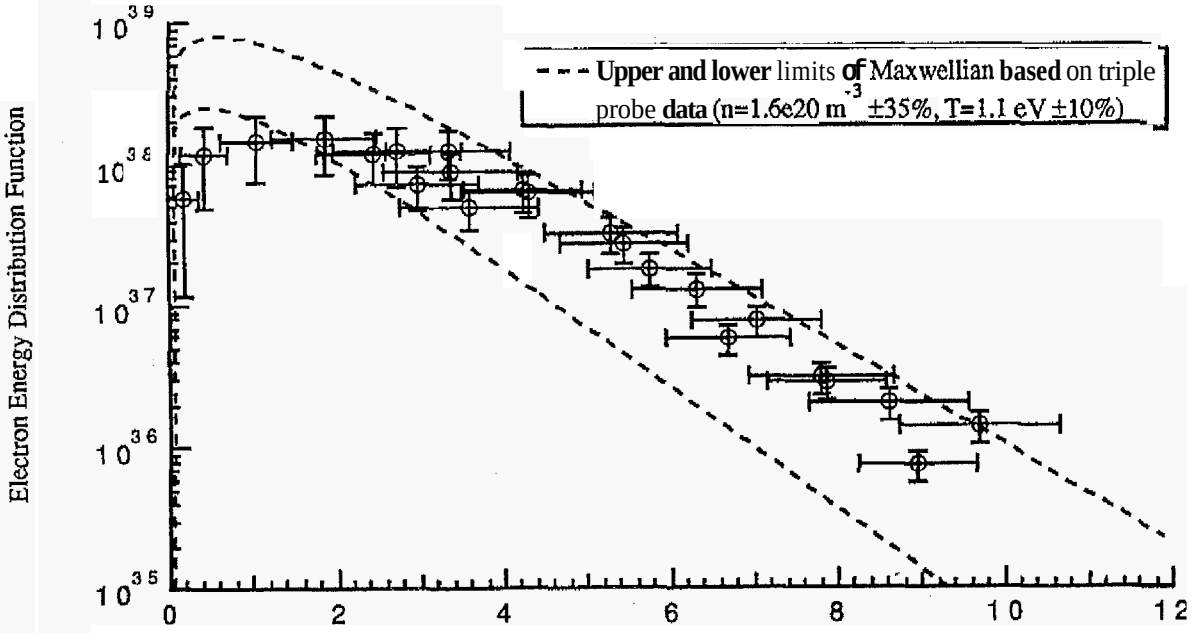


Figure 10. Non-normalized electron **energy distribution function for** $\xi = 0.27$, 16 g/s argon.

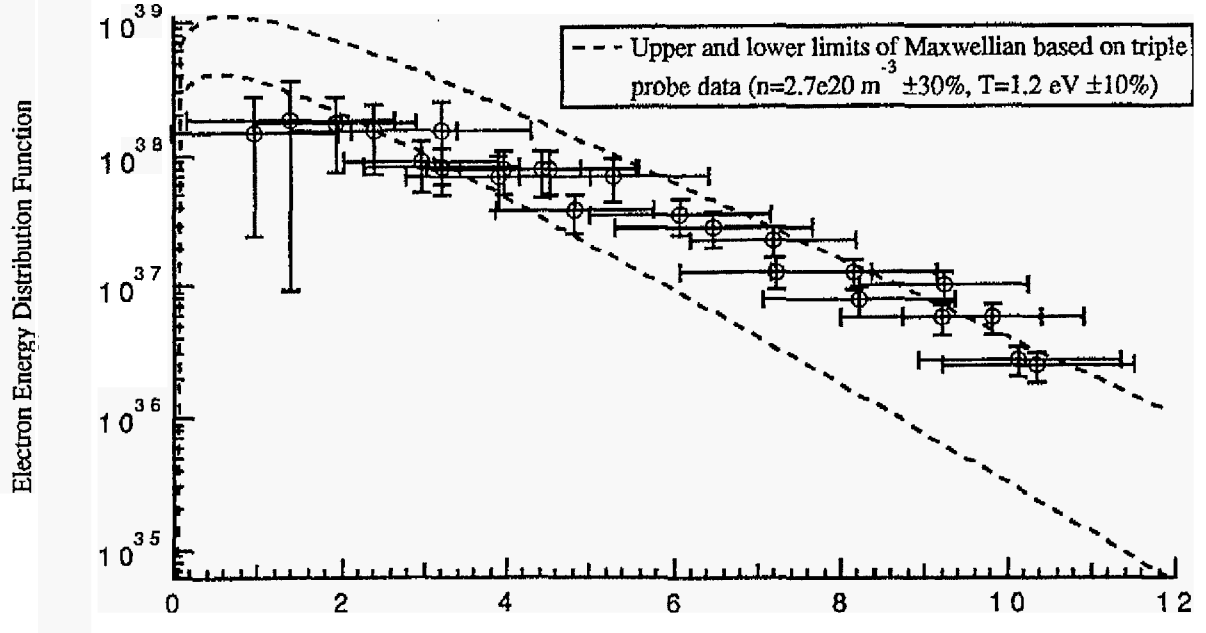


**Figure 11.** Non-normalized **electron energy distribution** function for $\xi = 0.41$, 16 g/s argon.

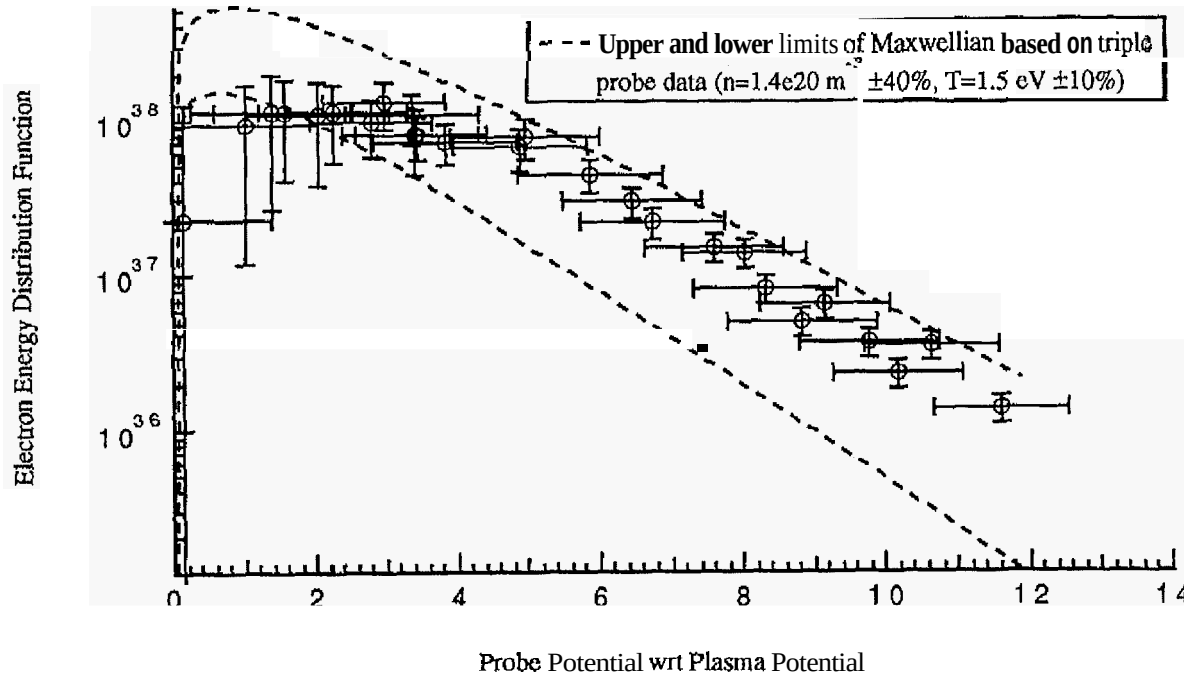


Figure 12. Non-normalized electron energy distribution function for $\xi = 0.44$, 6 g/s argon.